A Discrete/Continuous Minimization Method In Interferometric Image Processing*

José M. B. Dias and José M. N. Leitão

Instituto de Telecomunicações,
Instituto Superior Técnico,
1049-001 Lisboa, PORTUGAL
bioucas@lx.it.pt

Abstract. The 2D absolute phase estimation problem, in interferometric applications, is to infer absolute phase (not simply modulo-2π) from incomplete, noisy, and modulo-2π image observations. This is known to be a hard problem as the observation mechanism is nonlinear. In this paper we adopt the Bayesian approach. The observation density is 2π-periodic and accounts for the observation noise; the *a priori* probability of the absolute phase is modeled by a first order noncausal *Gauss Markov random field* (GMRF) tailored to smooth absolute phase images. We propose an iterative scheme for the computation of the *maximum a posteriori probability* (MAP) estimate. Each iteration embodies a discrete optimization step ($\mathbb{Z}$-step), implemented by network programming techniques, and an *iterative conditional modes* (ICM) step (π-step). Accordingly, we name the algorithm $\mathbb{Z}\pi$M, where letter M stands for maximization. A set of experimental results, comparing the proposed algorithm with other techniques, illustrates the effectiveness of the proposed method.

1 Introduction

In many classes of imaging techniques involving wave propagation, there is need for estimating absolute phase from incomplete, noisy, and modulo-2π observations, as the absolute phase is related with some physical entity of interest. Some relevant examples are [1] synthetic aperture radar, synthetic aperture sonar, magnetic resonance imaging systems, optical interferometry, and diffraction tomography.

In all the applications above referred the observed data relates with the absolute phase in a nonlinear and noisy way; the nonlinearity is sinusoidal and it is closely related with the wave propagation phenomena involved in the acquisition process; noise is introduced both by the acquisition process and by the electronic equipment. Therefore, the absolute phase should be inferred (*unwrapped* in the interfermetric jargon) from noisy and modulo-2π observations (the so-called *principal phase values* or *interferogram*).

* This work was supported by the Fundação para a Ciência e Tecnologia, under the project POSI/34071/CPS/2000.

Broadly speaking, absolute phase estimation methods can be classified into four major classes: path following methods, minimum-norm methods, Bayesian and regularization methods, and parametric models. Thesis [2] and paper [3] provide a comprehensive account of these methods.

The mainstream of absolute phase estimation research in interferometry takes a two step approach: in the first step, a filtered interferogram is inferred from noisy images; in the second step, the phase is unwrapped by determining the 2π multiples. Path following and minimum-norm schemes are representative of this approach (see [1] for comprehensive description of these methods). The main drawback of these methods is that the filtering process destroys the modulo-2π information in areas of high phase rate.

In a quite different vein, and recognizing that the absolute phase estimation is an ill-posed problem, papers [4], [5], [6], [7] have adopted the regularization framework to impose smoothness on the solution. The same objective has been pursued in papers [8], [9], [10], [11] by adopting a Bayesian viewpoint. Papers [8], [9] apply a nonlinear recursive filtering technique to determine the absolute phase. Paper [10] considers an InSAR (interferometric synthetic aperture radar) observation model taking into account not only the image absolute phase, but also the *backscattering coefficient* and the *correlation factor* images, which are jointly recovered from InSAR image pairs. Paper [11] proposes a fractal based prior and the simulated annealing scheme to compute the absolute phase image.

Parametric models constrain the absolute phase to belong to a given parametric model. Works [12], [13] have adopted low order polynomials. These approaches yields good results if the low order polynomials represent accurately the absolute phase. However, in practical applications the entire phase function cannot be approximated by a single 2-D polynomial model. To circumvent model mismatches, work [12] proposes a partition of the observed field where each partition element has its own model.

1.1 Proposed Approach

We adopt the Bayesian viewpoint. The likelihood function, which models the observation mechanism given the absolute phase, is 2π-periodic and accounts for the interferometric noise. The *a priori* probability of the absolute phase is modeled by a first order noncausal Gauss Markov random field (GMRF) [14], [15] tailored to smooth fields.

Papers [8], [9], [10] have also followed a Bayesian approach to absolute phase estimation. The prior therein used was a first order causal GMRF. Taking advantage of this prior and using the *reduced order model* (ROM) [16] approximation of the GMRF, the absolute was estimated with a nonlinear recursive filtering technique. Compared with the present approach, the main difference concerns the prior: we use a first order noncausal GMRF prior. In terms of estimation, the noncausal prior has implicit a batch perspective, where the absolute phase estimate at each site is based on the complete observed image. This is in contrast with the recursive filtering technique [8], [9], [10], where the absolute phase

estimate of a given site is inferred only from past (in the lexicographic sense) observed data.

To the computation of the MAP estimate, we propose an iterative procedure with two steps per iteration: the first step, termed $\mathbb{Z}$-step, maximizes the posterior density with respect to the field of 2π phase multiples; the second step, termed π-step, maximizes the posterior density with respect to the phase principal values. $\mathbb{Z}$-step is a discrete optimization problem solved by network programming techniques. π-step is a continuous optimization problem solved approximately by the *iterated conditional modes* (ICM) [17] scheme. We term our algorithm $\mathbb{Z}\pi$M, where the letter M stands for maximization.

The paper is organized as follows. Section 2 introduces the observation model, the first order noncausal GMRF prior, and the posteriori density. Section 3 elaborates on the estimation procedure. Namely, we derive solutions for the $\mathbb{Z}$-step and for the π-step. Section 4 presents results.

2 Adopted Models

2.1 Observation Model

The complex envelop of the signal read by the receiver from a given site is given by

$$x = e^{-j\phi} + n, \tag{1}$$

where ϕ is the phase to be estimated and n is complex zero-mean circular Gaussian noise. Model (1), adopted in papers [8] and [9], applies, for example, to laser interferometry [18].

Defining $\sigma_n^2 \equiv E[|n|^2]$, the probability density function[1] of x is (see, e.g., [19, ch. 3])

$$p_{x|\phi}(x|\phi) = \frac{1}{\pi\sigma_n^2} \exp\left\{ -\frac{\left|x - e^{-j\phi}\right|^2}{\sigma_n^2} \right\}. \tag{2}$$

Developing the quadratic form in (2), one is led to

$$p_{x|\phi}(x|\phi) = ce^{\lambda\cos(\phi-\eta)}, \tag{3}$$

where $c = c(x, \sigma_n)$ and

$$\eta = \arg(x) \tag{4}$$

$$\lambda = \frac{|x|}{\sigma_n^2}. \tag{5}$$

The likelihood function $p_{x|\phi}(x|\phi)$ is 2π-periodic with respect to ϕ with maxima at $\phi = 2\pi k + \eta$, for $k \in \mathbb{Z}$ ($\mathbb{Z}$ denotes the integer set). Thus η is a maximum

[1] For compactness, lowercase letters will denote random variables and their values as well.

likelihood estimate of ϕ. The peakiness of the maxima of (3), controlled by parameter λ, is an indication of how trustful data is.

The observation model (1) does not apply to applications exhibiting speckle noise such as synthetic apertura radar and synthetic aperture sonar. We have shown in [10], however, that the observation model of these applications leads to an observation density with the same formal structure given by formula (3).

Let $\boldsymbol{\phi} \equiv \{\phi_{ij} \,|\, (i,j) \in Z\}$ and $\mathbf{x} \equiv \{x_{ij} \,|\, (i,j) \in Z\}$ denote the absolute phase and complex amplitude associated to sites $Z \equiv \{(i,j) |\, i,j = 1,\ldots,N\}$ (we assume without lack of generality that images are squared). Assuming that the components of $\mathbf{x}$ are conditionally independent,

$$p_{\mathbf{x}|\phi}(\mathbf{x}|\boldsymbol{\phi}) = \prod_{ij \in Z} p_{x_{ij}|\phi_{ij}}(x_{ij}|\phi_{ij}). \tag{6}$$

The conditional independence assumption is valid if the resolution cells associated to any pair of pixels are disjoint. Usually this is a good approximation, since the *point spread function* of the imaging systems is only slightly larger than the corresponding inter-pixel distance (see [20]).

2.2 Prior Model

Image $\boldsymbol{\phi}$ is assumed to be smooth. *Gauss-Markov random fields* [14], [15] are both mathematically and computationally suitable for representing local interactions, namely to impose smoothness. We take the *first order* noncausal GMRF

$$p_{\phi}(\boldsymbol{\phi}) \propto \exp\left\{ -\frac{\mu}{2} \sum_{ij \in Z_1} (\Delta\phi^h_{ij})^2 + (\Delta\phi^v_{ij})^2 \right\}, \tag{7}$$

where $\Delta\phi^h_{ij} \equiv (\phi_{ij} - \phi_{i,j-1})$, $\Delta\phi^v_{ij} \equiv (\phi_{ij} - \phi_{i-1,j})$, $Z_1 \equiv \{(i,j) |\, i,j = 2,\ldots,N\}$, and μ^{-1} means the variance of increments $\Delta\phi^h_{ij}$ and $\Delta\phi^v_{ij}$.

2.3 Posterior Density

Invoking the Bayes rule, we obtain the posterior probability density function of $\boldsymbol{\phi}$, given $\mathbf{x}$, as

$$p_{\phi|\mathbf{x}}(\boldsymbol{\phi}|\mathbf{x}) \propto p_{\mathbf{x}|\phi}(\mathbf{x}|\boldsymbol{\phi}) p_{\phi}(\boldsymbol{\phi}), \tag{8}$$

where the factors not depending on $\boldsymbol{\phi}$ were discarded. Introducing (6) and (7) into (8), we obtain

$$p_{\phi|\mathbf{x}}(\boldsymbol{\phi}|\mathbf{x}) \propto e^{\sum_{ij \in Z} \lambda_{ij} \cos(\phi_{ij} - \eta_{ij}) - \frac{\mu}{2} \sum_{ij \in Z_1} (\Delta\phi^h_{ij})^2 + (\Delta\phi^v_{ij})^2}. \tag{9}$$

The posterior distribution (9) is assumed to contain all information one needs to compute the absolute phase estimate $\widehat{\boldsymbol{\phi}}$.

3 Estimation Procedure

The MAP criterion is adopted for computing $\widehat{\boldsymbol{\phi}}$. Accordingly,

$$\widehat{\boldsymbol{\phi}}_{MAP} = \arg\max_{\boldsymbol{\phi}} p_{\boldsymbol{\phi}|\mathbf{x}}(\boldsymbol{\phi}|\mathbf{x}). \tag{10}$$

Due to the periodic structure of $p_{x|\phi}(x|\phi)$, computing the MAP solution leads to a huge non-convex optimization problem, with unbearable computation burden. Instead of computing the exact estimate $\widehat{\boldsymbol{\phi}}_{MAP}$, we resort to a suboptimal scheme that delivers nearly optimal estimates, with a far less computational load.

Let the absolute phase ϕ_{ij} be uniquely decomposed as

$$\phi_{ij} = \psi_{ij} + 2\pi k_{ij}, \tag{11}$$

where $k_{ij} = \lfloor(\phi_{ij} + \pi)/(2\pi)\rfloor \in \mathbb{Z}$ is the so-called wrap-count component of ϕ_{ij}, and $\psi_{ij} \in [-\pi, \pi[$ is the principal value of ϕ_{ij}. The MAP estimate (10) can be rewritten in terms of $\boldsymbol{\psi} \equiv \{\psi_{ij} \,|\, (i,j) \in Z\}$ and $\mathbf{k} \equiv \{k_{ij} \,|\, (i,j) \in Z\}$ as

$$(\widehat{\boldsymbol{\psi}}_{MAP}, \widehat{\mathbf{k}}_{MAP}) = \arg\max_{\boldsymbol{\psi},\mathbf{k}} p_{\boldsymbol{\phi}|\mathbf{x}}(\boldsymbol{\psi} + 2\pi\mathbf{k}|\mathbf{x}) \tag{12}$$

$$= \arg\left\{\max_{\boldsymbol{\psi}}\left\{\max_{\mathbf{k}} p_{\boldsymbol{\phi}|\mathbf{x}}(\boldsymbol{\psi} + 2\pi\mathbf{k}|\mathbf{x})\right\}\right\}. \tag{13}$$

Instead of computing (13), we propose a procedure that successively and iteratively maximizes $p_{\boldsymbol{\phi}|\mathbf{x}}(\boldsymbol{\psi} + 2\pi\mathbf{k}|\mathbf{x})$ with respect to $\mathbf{k} \in \mathbb{Z}^{N^2}$ and $\boldsymbol{\psi} \in [-\pi, \pi[^{N^2}$. We term this maximization on the sets $\mathbb{Z}$ and $[-\pi, \pi[$ as the $\mathbb{Z}\pi$M algorithm; Fig. 1 shows the corresponding pseudo-code.

Initialization: $\widehat{\boldsymbol{\psi}}^{(0)} = \boldsymbol{\eta}$
For $t = 1, 2, \ldots,$

Unwrapping step:

$$\widehat{\mathbf{k}}^{(t)} = \arg\max_{\mathbf{k}} p_{\boldsymbol{\phi}|\mathbf{x},\mathbf{I}}(\boldsymbol{\psi}^{(t-1)} + 2\pi\mathbf{k}|\mathbf{x}) \tag{14}$$

Smoothing step:

$$\widehat{\boldsymbol{\psi}}^{(t)} = \arg\max_{\boldsymbol{\psi}} p_{\boldsymbol{\phi}|\mathbf{x},\mathbf{I}}(\boldsymbol{\psi} + 2\pi\mathbf{k}^{(t)}|\mathbf{x}) \tag{15}$$

Termination test:

If $[p_{\boldsymbol{\phi}|\mathbf{x},\mathbf{I}}(\widehat{\boldsymbol{\phi}}^{(t)}|\mathbf{x}) - p_{\boldsymbol{\phi}|\mathbf{x},\mathbf{I}}(\widehat{\boldsymbol{\phi}}^{(t-1)}|\mathbf{x})] < \xi$
break loop for

Fig. 1. $\mathbb{Z}\pi$**M** Algorithm.

The $\mathbb{Z}\pi$M algorithm is greedy, since the posterior density $p_{\boldsymbol{\phi}|\mathbf{x}}(\boldsymbol{\phi}|\mathbf{x})$ can not decrease in each step of the each iteration. Thus, the stationary points of the

couple (14)-(15) correspond to local maxima of $p_{\phi|\mathbf{x}}(\boldsymbol{\phi}|\mathbf{x})$. Nevertheless, the proposed method yields systematically good results, as we will show in next section.

The unwrapping step (14) finds the maximum of the posterior density $p_{\phi|\mathbf{x}}(\boldsymbol{\phi}|\mathbf{x})$ on a mesh obtained by discretizing each coordinate ϕ_{ij} according to (11). The first estimate $\widehat{\mathbf{k}}^{(1)}$ delivered by the unwrapping step is based on the maximum likelihood estimate $\boldsymbol{\eta} \equiv \{\eta_{ij} \,|\, (i,j) \in Z\}$. Smoothing is implemented by the π-step (15). This is in contrast with the scheme followed by most phase unwrapping algorithms, where the phase is estimated with basis on on a smooth version of $\boldsymbol{\eta}$, under the assumption that the phase ϕ is constant within windows of given size. This assumption leads to strong errors in areas of high phase rate.

3.1 $\mathbb{Z}$-Step

Since the logarithm is strictly increasing and $\cos(\psi_{ij} + 2\pi k_{ij} - \eta_{ij})$ does not depend on k_{ij}, solving the maximization step (14) is equivalent to solve

$$\widehat{\mathbf{k}} = \arg\min_{\mathbf{k}} E(\mathbf{k}|\boldsymbol{\psi}), \tag{16}$$

where the energy $E(\mathbf{k}|\boldsymbol{\psi})$ is given by

$$E(\mathbf{k}|\boldsymbol{\psi}) \equiv \sum_{ij \in Z_1} (\Delta\phi^h_{ij})^2 + (\Delta\phi^v_{ij})^2, \tag{17}$$

with

$$\Delta\phi^h_{ij} = [2\pi(k_{ij} - k_{i,j-1}) - \Delta\psi^h_{ij}] \tag{18}$$
$$\Delta\phi^v_{ij} = [2\pi(k_{ij} - k_{i-1,j}) - \Delta\psi^v_{ij}], \tag{19}$$

and $\Delta\psi^h_{ij} = \psi_{i,j-1} - \psi_{ij}$ and $\Delta\psi^v_{ij} = \psi_{i-1,j} - \psi_{ij}$.

A simple but lengthy manipulation of equation (17) allows us to write

$$\widehat{\bar{\mathbf{k}}} = \arg\min_{\bar{\mathbf{k}} \in \mathbb{Z}^{N^2}} (\bar{\mathbf{k}} - \bar{\mathbf{k}}_0)^T \mathbf{A} (\bar{\mathbf{k}} - \bar{\mathbf{k}}_0), \tag{20}$$

where the column vector $\bar{\mathbf{k}}$ is the column by column stacking of matrix $\mathbf{k}$, matrix $\mathbf{A}$ is nonnegative block Toeplitz and symmetric, and vector $\mathbf{k}_0$ depends on $\Delta\psi^h_{ij}$ and $\Delta\psi^v_{ij}$. For nonnegative symmetric matrices $\mathbf{A}$, the integer least square problem (20) is known as the *nearest lattice vector problem* and it is NP-hard [21]. It arises, for example, in highly accurate positioning by Global Positionning System (GPS) [22], [23]. Works [24], [21], [22] propose suboptimal polynomial time algorithms for finding an approximatly nearest lattice solution.

In our case, energy $E(\mathbf{k}|\boldsymbol{\psi})$ is a sum of quadratic functions of $(k_{ij} - k_{i-1,j})$ and $(k_{ij} - k_{i,j-1})$. This is a special case of a nearest lattice vector problem, for which we propose a network programming algorithm that finds the exact solution in polynomial time. The algorithm is inspired in the Flyn's minimum discontinuity approach [25], which minimizes the sum of $|\lfloor \Delta\phi^h_{ij} + \pi \rfloor|$ and $|\lfloor \Delta\phi^v_{ij} + \pi \rfloor|$,

where $\lfloor x \rfloor$ denotes the hightest integer lower than x. Flyn's objective function is, therefore, quite different from ours. However, both objective functions are the sum of first order click potentials depending only on $\Delta\phi^h_{ij}$, and $\Delta\phi^v_{ij}$. This structural similarity allows us to adapt Flyn's ideas to our problem.

The following lemma assures that if the minimum of $E(\mathbf{k}|\boldsymbol{\psi})$ is not yet reached, then there exists a binary image $\delta\mathbf{k}$ (i.e., the elements of $\delta\mathbf{k}$ are all 0 or 1) such that $E(\mathbf{k}+\delta\mathbf{k}|\boldsymbol{\psi}) < E(\mathbf{k}|\boldsymbol{\psi})$.

Lemma 1 *Let* $\mathbf{k}_1$ *and* $\mathbf{k}_2$ *be two wrap-count images such that*

$$E(\mathbf{k_2}|\boldsymbol{\psi}) < E(\mathbf{k_1}|\boldsymbol{\psi}). \tag{21}$$

Then, there exists a binary image $\delta\mathbf{k}$ *such that*

$$E(\mathbf{k_1}+\delta\mathbf{k}|\boldsymbol{\psi}) < E(\mathbf{k}_1|\boldsymbol{\psi}). \tag{22}$$

Proof. See [26].

According to Lemma 1, we can iteratively compute $\mathbf{k}_i = \mathbf{k}_{i-1} + \delta\mathbf{k}$, where $\delta\mathbf{k} \in \{0,1\}^{N^2}$ minimizes $E(\mathbf{k}_{i-1}+\delta\mathbf{k}|\boldsymbol{\psi})$, until the the minimum energy is reached. Each minimization is a discrete optimization problem that can be exactly solved in polynomial time by using network programming techniques such as maximum flow [27] or minimum cut [28]. We note however that, in the iterative scheme just described, it is not necessary to compute the exact minimizer of $E(\mathbf{k}_{i-1}+\delta\mathbf{k}|\boldsymbol{\psi})$ with respect to $\delta\mathbf{k}$, but only a binary image $\delta\mathbf{k}$ that decreases $E(\mathbf{k}_{i-1}+\delta\mathbf{k}|\boldsymbol{\psi})$. Based on this fact we propose an efficient algorithm that iteratively search for improving binary images $\delta\mathbf{k}$.

The following lemma, presented and proofed in the appendix of [25], assures that if there exists an improving binary image $\delta\mathbf{k}$ [i.e., $E(\mathbf{k}+\delta\mathbf{k}|\boldsymbol{\psi}) < E(\mathbf{k}|\boldsymbol{\psi})$], then there exists another improving binary image $\delta\mathbf{l}$ such that the sets $S_1(\delta\mathbf{l}) \equiv \{(i,j) \in Z \,|\, \delta l_{ij} = 1\}$ and $S_0(\delta\mathbf{l}) \equiv \{(i,j) \in Z \,|\, \delta l_{ij} = 0\}$ are both connected in the first order neighborhood sense; i.e., given two sites s_1 and s_n of S_1 (S_0), there exists a sequence of first order neighbors, all in S_1 (S_0), that begins in s_1 and ends in s_n. We call images $\delta\mathbf{l}$ with this property, binary partitions of Z.

Lemma 2 *Suppose that there exits a binary image* $\delta\mathbf{k}$ *such that*

$$E(\mathbf{k}+\delta\mathbf{k}|\boldsymbol{\psi}) < E(\mathbf{k}|\boldsymbol{\psi}).$$

Then there exists a binary partition of Z, $\delta\mathbf{l}$, *such that*

$$E(\mathbf{k}+\delta\mathbf{l}|\boldsymbol{\psi}) < E(\mathbf{k}|\boldsymbol{\psi}).$$

Proof. See Lemma 2 in the appendix of [25].

Flyn's central idea is to search for improving binary partitions $\delta\mathbf{l}$ [termed in [25] an elementary operation (EO)]. Once $\delta\mathbf{l}$ is found the wrap-count image $\mathbf{k}$ is updated to $\mathbf{k}+\delta\mathbf{l}$. If no EO is possible then, according to Lemma 2, energy $E(\mathbf{k}|\boldsymbol{\psi})$

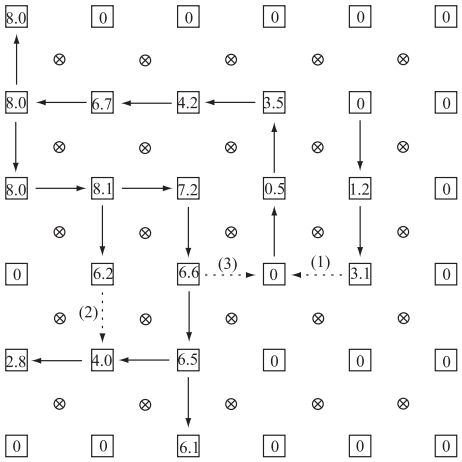

Fig. 2. Auxiliary graph to implement Flyn's algorithm (squared nodes) interleaved with phase sites (circled and crossed nodes). A leftward (rightward) edge indicates an unit increment of the wrap-count below (above) the edge. A downward (upward) edge indicates an unit increment of the wrap-count right (left) to the edge.

can not be decreased by any binary image increment of the actual argument $\mathbf{k}$. Thus, by Lemma 1, $E(\mathbf{k}|\boldsymbol{\psi})$ has reached its minimum.

To check if a given binary partition $\delta\mathbf{l}$ improves the energy, one has to compute only those click potentials of $E(\mathbf{k}|\boldsymbol{\psi})$ containing sites on both sets $S_1(\delta\mathbf{l})$ and $S_0(\delta\mathbf{l})$; i.e., one has to compute click potentials of $E(\mathbf{k}|\boldsymbol{\psi})$ only along loops (this is still true on the boundary of Z by taking zero potentials). The Flyn's algorithm uses graph theory techniques to represent and generate EOs. Figure 2 shows an auxiliary graph, whose nodes are interleaved with the phase sites. The edges sign which wrap-counts are to be incremented: a leftward (rightward) edge indicates an unit increment of the wrap-count below (above) the edge. A downward (upward) edge indicates a unit increment of the wrap-count right (left) to the edge. The algorithm works by creating and extending paths made of directed edges. When a path is extended to form a loop, the algorithm performs an EO, removes the loop from the collection of paths and resumes the path extension.

Assume that the array of auxiliary nodes has indexes in the set $\{(i,j)\,|\,i,j = 1,\ldots,N+1\}$. Define the cost of an edge $\delta V(i,j;i',j')$ between the first order neighbors (i',j') and (i,j) as $E(\mathbf{k}|\boldsymbol{\psi}) - E(\mathbf{k}+\delta\mathbf{k}|\boldsymbol{\psi})$, where $\delta\mathbf{k}$ is the wrap-count increment induced by the edge. With this definitions and having in attention the structure of $E(\mathbf{k}|\boldsymbol{\psi})$ [see (17)], we are led to

$$\begin{aligned}
\delta V(i,j;i,j-1) &= -4\pi(\pi + \Delta\phi^v_{i,j-1})\bar{h}_{i,j-1}\\
\delta V(i,j-1;i,j) &= -4\pi(\pi - \Delta\phi^v_{i,j-1})\bar{h}_{i,j-1}\\
\delta V(i-1,j;i,j) &= -4\pi(\pi + \Delta\phi^h_{i-1,j})\bar{v}_{i-1,j}\\
\delta V(i,j;i-1,j) &= -4\pi(\pi - \Delta\phi^h_{i-1,j})\bar{v}_{i-1,j}.
\end{aligned}$$

The values of boundary edges are defined to be zero; i.e., $\delta V(1,j) = \delta V(N+1,j) = \delta V(i,1) = \delta V(i,N+1) = 0$.

Figure 2 represents the state of the graph at a given instant. Assuming that there are no loops, the set of edges defines a given number of trees. The value of each node, $V(i,j)$, is the sum of edge values corresponding to the path between the node and the tree root. In Figure 2 there are two trees. We stress that the node values are real numbers, whereas in the Flyn's algorithm they are integers. The reason is that our energy $E(\mathbf{k}|\boldsymbol{\psi})$ takes values in the non-negative reals while the Flyn's energy takes values on the positive integers.

The basic step of Flyn's algorithm is to revise the set of paths by adding a new edge. An edge from (i,j) to a first order neighbor (i',j'), if not presented, is added if

$$\Delta V \equiv V(i,j) + \delta V(i,j;i',j') - V(i',j') > 0.$$

If $\Delta V \leq 0$ then the new path to (i',j') would have a negative or zero value or would fail to improve an existing path. If the edge is added the set of paths is revised in one of the three possible ways (a minor modification of [25]): 1) edge addition, 2) edge replacement, and 3) edge completion.

The dashed edges in Fig. 2 illustrate graph revision of type 1, 2, and 3. For a more detailed example, see Flyn's paper [25].

The algorithm alternates between type 1 and type 2 revisions until a loop is found, performing then a type 3 revision. If for any attempt of edge addition $\Delta V \leq 0$, then no loop completion is possible and, according to Lemma 2 and Lemma 1, the algorithm terminates.

Flyn's algorithm [25] and Costantini's [29] algorithm are equivalent, as they minimize the L^1 norm. Costantini has shown that L^1 minimization is equivalent to finding the minimum cost flow on a given directed network. Minimum cost flow is a graph problem for which there exists efficient solutions (see, e.g. [30]). We do not implement our $\mathbb{Z}$-step using Costantini's solution because the graph can not be used with L^p norm for $p \neq 1$.

Another alternative to implement the $\mathbb{Z}$-step might be the discrete optimization scheme proposed in [31]. Authors of this paper claim that their approach, based on the maximum flow algorithm applied to a suitable graph, minimizes any energy function in which the smoothness term is convex and involves only pairs of neighboring pixels. However, the graph for a given convex smoothness function is not presented in [31].

3.2 Smoothing Step

The smoothing step (15) amounts to compute $\widehat{\boldsymbol{\psi}}$ given by

$$\widehat{\boldsymbol{\psi}} = \arg \max_{\boldsymbol{\psi} \in [-\pi,\pi[^{N^2}} \sum_{ij \in Z} \lambda_{ij} \cos(\phi_{ij} - \eta_{ij}) - \frac{\mu}{2} \sum_{ij \in Z_1} (\Delta\phi^h_{ij})^2 + (\Delta\phi^v_{ij})^2, \quad (23)$$

where $\phi_{ij} = 2\pi k_{ij} + \psi_{ij}$. The function to be maximized in (23) is not convex due to terms $\lambda_{ij}\cos(\phi_{ij} - \eta_{ij})$. Computing $\widehat{\boldsymbol{\psi}}$ is therefore a hard problem. Herein, we

adopt the ICM approach [14], which, in spite of being suboptimal, yields good results for the problem at hand.

ICM is a coordinatewise ascent technique where all coordinates are visited according to a given schedule. After some simple algebraic manipulation of the objective function (23), we conclude that its maximum with respect to ψ_{ij} is given by

$$\widehat{\psi}_{ij} = \arg \max_{\psi_{ij} \in [-\pi, \pi[} \left\{ \beta_{ij} \cos(\psi_{ij} - \eta_{ij}) - (\psi_{ij} - \bar{\psi}_{ij})^2 \right\}, \tag{24}$$

where

$$\beta_{ij} = \frac{\lambda_{ij}}{2\mu} \tag{25}$$

$$\bar{\psi}_{ij} = \bar{\phi}_{ij} - 2\pi k_{ij} \tag{26}$$

$$\bar{\phi}_{ij} = \frac{\phi_{i-1,j} + \phi_{i,j-1} + \phi_{i+1,j} + \phi_{i,j+1}}{4}. \tag{27}$$

There are no closed form solutions for maximization (24), since it involves transcendent and power functions. We compute $\widehat{\psi}_{ij}$ using a simple two-resolution numeric method. First we search $\widehat{\psi}_{ij}$ in the set $\{\pi i/M \,|\, i = -M, \ldots, M-1\}$. Next we refine the search by using the set $\{\pi i_0/M + \pi i/M^2 \,|\, i = -M, \ldots, M-1\}$, where $\pi i_0/M$ is the result of the first search. We have used $M = 20$, which leads to the maximum error of $\pi/(20)^2$.

Phase estimate $\widehat{\psi}_{ij}$ depends in a nonlinear way on data η_{ij} and on the mean weighted phase $\bar{\psi}_{ij}$. The balance between these two components is controlled by parameter β_{ij}. Assuming that $|\widehat{\psi}_{ij} - \eta_{ij}| \ll \pi$, then $\cos(\psi_{ij} - \eta_{ij})$ is well approximated by the quadratic form $1 - (\psi_{ij} - \eta_{ij})^2/2$, thus leading to the linear approximation

$$\widehat{\psi}_{ij} \simeq \frac{\beta_{ij}\eta_{ij} + 2\bar{\psi}_{ij}}{\beta_{ij} + 2}. \tag{28}$$

Reintroducing (28) in the above condition, one gets $|\bar{\psi}_{ij} - \eta_{ij}| \ll 2\pi/(\beta_{ij} + 2)$. If this condition is not met, the solution becomes highly nonlinear on η_{ij} and $\bar{\psi}_{ij}$: as $|\bar{\psi}_{ij} - \eta_{ij}|$ increases, at some point the phase $\widehat{\psi}_{ij}$ becomes thresholded to $\pm\pi$, being therefore independent of the observed data η_{ij}.

Concerning computer complexity the $\mathbb{Z}$-step is, by far, the most demanding one, using a number of floating point operations very close to the Flyn's minimum discontinuity algorithm. Since the proposed scheme needs roughly four $\mathbb{Z}$-steps, is has, approximately 4 times the Flyn's minimum discontinuity algorithm complexity. To our knowledge there is no formula for the Flyn's algorithm complexity (see remarks about complexity in [25]). Nevertheless, we have found, empirically, a complexity of approximately $O(N^3)$ for the $\mathbb{Z}$-step.

4 Experimental Results

The algorithm derived in the previous sections is now applied to synthetic data.

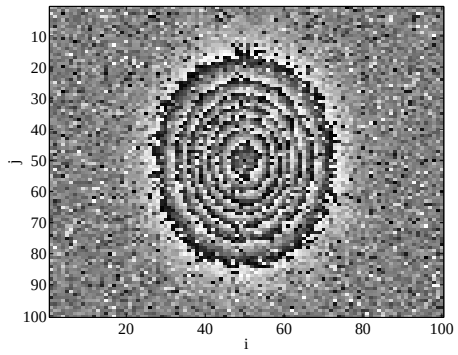

Fig. 3. Interfergram ($\boldsymbol{\eta}$-image) of a Gaussian elevation of height 14π rad and standard deviations $\sigma_i = 10$ and $\sigma_j = 15$ pixels. The noise variance is $\sigma_n = 1.05$.

Figure 3 displays the interferogram ($\boldsymbol{\eta} = \{\eta_{ij}\}$ image) generated according to density (2) with noise variance $\sigma_n = 1.05$. The absolute phase image $\boldsymbol{\phi}$ is a Gaussian elevation of height 14π rad and standard deviations $\sigma_i = 10$ and $\sigma_j = 15$ pixels. The magnitude of the phase difference $\phi_{i,j+1} - \phi_{ij}$ takes the maximum value of 2.5 and is greater than 2 in many sites. On the other hand a noise variance of $\sigma_n = 1.05$ implies a standard deviation the maximum likelihood estimate η_{ij} of 0.91. This figure is computed with basis on the density of η obtained from the joint density (2). In these conditions, the task of absolute phase estimation is extremely hard, as the interferogram exhibits a large number of inconsistencies; i.e., the observed image $\boldsymbol{\eta}$ is not consistent with the assumption of absolute phase differences less than π in a large number of sites. In the unwrapping jargon the interferogram is said to have a lot of residues.

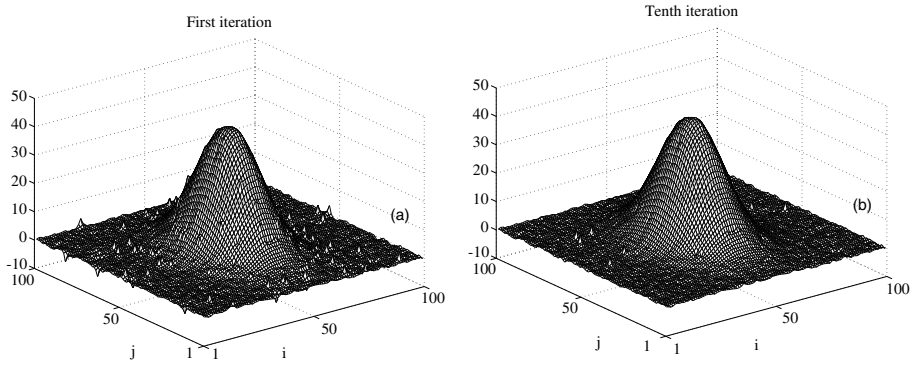

Fig. 4. Phase estimate $\widehat{\boldsymbol{\phi}}^{(t)}$; (a) $t = 1$; (b) $t = 10$.

The smoothness parameter was set to $\mu = 1/0.8^2$, thus modelling phase images with phase differences (horizontal and vertical) of standard deviation 0.8. This value is too large for most of the true absolute phase image $\boldsymbol{\phi}$ and too small for sites in the neighborhood of sites $(i = -45, j = 50)$ and $(i = 55, j = 50)$ (where the magnitude of the phase difference has its largest value). Nevertheless, the $\mathbb{Z}\pi$M algorithm yields good results as it can be read from Fig. 4; Fig. 4(a) shows the phase estimate $\widehat{\boldsymbol{\phi}}^{(1)}$ and Fig. 4(b) shows the phase estimate $\widehat{\boldsymbol{\phi}}^{(10)}$.

Figure 5 plots the logarithm of the posterior density $\ln p_{\phi|\mathbf{x}}(\widehat{\boldsymbol{\phi}}^{(t)}|\mathbf{x})$ and the L^2 norm of the estimation error $\|\widehat{\boldsymbol{\phi}} - \boldsymbol{\phi}\|^2 \equiv N^{-2} \sum_{ij} (\widehat{\phi}_{ij} - \phi_{ij})^2$ as function of the iteration t. The four non-integers ticked between two consecutive integers refer to four consecutive ICM sweeps, implementing the π-step of the $\mathbb{Z}\pi$M algorithm. Notice that the larger increment in $\ln p_{\phi|\mathbf{x}}(\widehat{\boldsymbol{\phi}}^{(t)}|\mathbf{x})$ happens in both steps of the first iteration. For $t \geq 2$ only the $\mathbb{Z}$-step produces noticeable increments in the posterior density. These increments are however possible due to the very small increments produced by the smoothing steep. For $t > 4$ there is practically no improvement in the estimates.

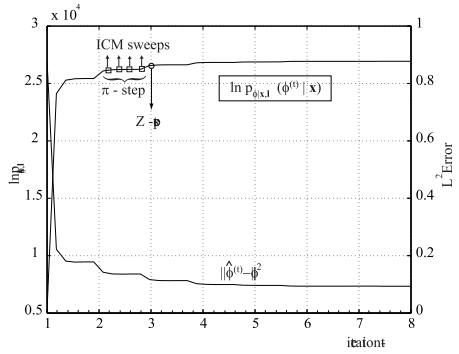

Fig. 5. Evolution of the logarithm of the posterior density $\ln p_{\phi|\mathbf{x}}(\widehat{\boldsymbol{\phi}}^{(t)}|\mathbf{x})$ and of the L^2 norm of the estimation error as function of the iteration t. $\mathbb{Z}$-steps coincide with integers, whereas ICM sweeps implementing π-step are assigned to the non-integer part of t.

To rank $\mathbb{Z}\pi$M algorithm, we have applied the following phase unwrapping algorithms to the present problem:

- **Path following type:** Golstein's branch cut (GBC) [32]; quality guided (QG) [33], [34]; and mask cut (MC) [35]
- **Minimum norm type:** Flyn's minimum discontinuity (FMD) [25]; weighted least-square (WLS) [36], [37]; and L^0 norm (L0N) (see [1, ch. 5.5])
- **Bayesian type**: recursive nonlinear filters [9] and [10] (NLF).

Path following and minimum norm algorithms were implemented with the code supplied in the book [1], using the following settings: GBC (-dipole yes); QG,

MC, (-mode min_var -tsize 3); and WLS (-mode min_var -tsize 3, -thresh yes). We have used the unweighted versions of the FMD and L0N algorithms.

Table 1. L^2 norm of the estimation errors of $\mathbb{Z}\pi$M and other unwrapping algorithms. The left column plots results based of the the maximum likelihood estimate of $\boldsymbol{\eta}$ using a 3×3 rectangular window; the right column plots results based on the non-smooth $\boldsymbol{\eta}$ given by (4).

	$\|\widehat{\boldsymbol{\phi}} - \boldsymbol{\phi}\|^2$	
Algorithm	Smooth $\boldsymbol{\eta}$	Non-smooth $\boldsymbol{\eta}$
$\mathbb{Z}\pi$M	–	0.1
GBC	48.0	7.0
QG	10.0	2.2
MC	40.8	28.6
FMD	22.4	3.4
WLS	8.8	3.5
L0N	24.1	2.6
NLF	–	40.1

Table 1 displays the L^2 norm of the estimation error $||\widehat{\boldsymbol{\phi}} - \boldsymbol{\phi}||^2$ for each of the classic algorithm referred above. Results on the left column area based on the maximum likelihood estimate of $\boldsymbol{\eta}$ given by (4), using a 3×3 rectangular window. Results on the right column are based on the interferogram $\boldsymbol{\eta}$ without any smoothing. Apart from the proposed $\mathbb{Z}\pi$M scheme, all the algorithms have produced poor results, some of them catastrophic. The reasons depend on the class of algorithms and are are basically the following:

- in the path following and minimum norm methods the noise filtering is the first processing steep and is disconnected from the phase unwrapping process. The noise filtering assumes the phase to be constant within given windows. In data sets as the one at hand, this assumption is catastrophic, even using small windows. On the other hand, if the smoothing steep is not applied, even if algorithm is able to infer most of the 2π multiples, the observation noise is fully present in estimated phase
- the recursive nonlinear approaches [9] and [10] fails basically because they use only the past observed data, in the lexicographic sense, to infer the absolute phase.

5 Concluding Remarks

The paper presented an effective approach to absolute phase estimation in interferometric appliactions. The Bayesian standpoint was adopted. The likelihood function, which models the observation mechanism given the absolute phase, is 2π-periodic and accounts for interferometric noise. The *a priori* probability of the absolute phase is a noncausal first order Gauss Markov random field (GMRF).

We proposed an iterative procedure, with two steps per iteration, for the computation of the *maximum a posteriory probability* MAP estimate. The first step, termed $\mathbb{Z}$-step, maximizes the posterior density with respect to the 2π phase multiples; the second step, termed π-step, maximizes the posterior density with respect to the phase principal values. The $\mathbb{Z}$-step is a discrete optimization problem solved exactly by network programming techniques inspired by Flyn's *minimum discontinuity algorithm* [25]. The π-step is a continuous optimization problem solved approximately by the *iterated conditional modes* (ICM) procedure. We call the proposed algorithm $\mathbb{Z}\pi$M, where the letter M stands for maximization.

The $\mathbb{Z}\pi$M algorithm, resulting from a Bayesian approach, accounts for the observation noise in a model based fashion. More specifically, the observation mechanism takes into account electronic and decorrelation noises. This is a crucial feature that underlies the advantage of the $\mathbb{Z}\pi$M algorithm over path following and minimum-norm schemes, mainly in regions where the phase rate is close to π. In fact, these schemes split the absolute phase estimation problem into two separate steps: in the first step the noise in the interferogram is filtered by applying low-pass filtering; in the second step, termed phase unwrapping, the 2π phase multiples are computed. For high phase rate regions, the application of first step makes it impossible to recover the absolute phase, as the principal values estimates are of poor quality. This is in contrast with the $\mathbb{Z}\pi$M algorithm, where the first step, the $\mathbb{Z}$-step, is an unwrapping applied over the observed interferogram.

To evaluate the performance of the $\mathbb{Z}\pi$M algorithm, a Gaussian shaped surface whit high phase rate, and 0dB of signal to noise ratio was considered. We have compared the computed estimates with those provided by the best path following and minimum-norm schemes, namely the Golstein's branch cut, the quality guided, the Flyn's minimum discontinuity, the weighted least-square, and the L^0 norm. The proposed algorithm yields good results, performing better and in some cases much better than the s technique just referred.

Concerning computer complexity, the $\mathbb{Z}\pi$M algorithm takes, approximately, a number of floating point operations proportional to the 1.5 power of the number of pixels . By far, the $\mathbb{Z}$-step is the most demanding one, using a number of floating point operations very close to the Flyn's minimum discontinuity algorithm. Since the proposed scheme needs roughly four $\mathbb{Z}$-steps, is has, approximately 4 times the Flyn's minimum discontinuity algorithm complexity.

Concerning future developments, we foresee the integration of the principal phase values in the posterior density as a major research direction. If this goal would be attained then the wrapp-count image would be the only unknown of the obtained posterior density and, most important, there would be no need for iterativeness in estimating the wrapp-count image. After obtaining this image, the principal phase values could be obtained using the π-step of the $\mathbb{Z}\pi$M algorithm.

References

1. D. Ghiglia and M. Pritt. *Two-Dimentional Phase Unwrapping. Theory, Algorithms, and Software*. John Wiley & Sons, New York, 1998.
2. J. Strand. *Two-dimensional Phase Unwrapping with Applications*. PhD thesis, Department of Mathematics, Faculty of Mathematics and Natural Sciences, University of Bergen, 1999.
3. J. Strand, T. Taxt, and A. Jain. Two-dimensional phase-unwrapping using a two-dimensional least square method. *IEEE Transactions on Geoscience and Remote Sensing*, 82(3):375–386, March 1999.
4. J. Marroquin and M. Rivera. Quadratic regularization functionals for phase unwrapping. *Journal of the Optical Society of America*, 11(12):2393–2400, 1995.
5. L. Guerriero, G. Nico, G. Pasquariello, and S. Starmaglia. New regularization scheme for phase unwrapping. *Applied Optics*, 37(14):3053–3058, 1998.
6. M. Rivera, J. Marroquin, and R. Rodriguez-Vera. Fast algorithm for integrating inconsistent gradient fields. *Applied Optics*, 36(32):8381–8390, 1995.
7. M. Servin, J. Marroquin, D. Malacara, and F. Cuevas. Phase unwrapping with a regularized phase-tracking system. *Applied Optics*, 37(10):19171–1923, 1998.
8. J. Leitão and M. Figueiredo. Interferometric image reconstruction as a nonlinear Bayesian estimation problem. In *Proceedings of the First IEEE International Conference on Image Processing – ICIP'95*, volume 2, pages 453–456, 1995.
9. J. Leitão and M. Figueiredo. Absolute phase image reconstruction: A stochastic nonlinear filtering approach. *IEEE Transactions on Image Processing*, 7(6):868–882, June 1997.
10. J. Dias and J. Leitão. Simultaneous phase unwrapping and speckle smoothing in SAR images: A stochastic nonlinear filtering approach. In *EUSAR'98 European Conference on Synthetic Aperture Radar*, pages 373–377, Friedrichshafen, May 1998.
11. G. Nico, G. Palubinskas, and M. Datcu. Bayesian approach to phase unwrapping: theoretical study. *IEEE Transactions on Signal processing*, 48(9):2545–2556, Sept. 2000.
12. B. Friedlander and J. Francos. Model based phase unwrapping of 2-d signals. *IEEE Transactions on Signal Processing*, 44(12):2999–3007, 1996.
13. Z. Liang. A model-based for phase unwrapping. *IEEE Transactions on Medical Imaging*, 15(6):893–897, 1996.
14. J. Besag. On the statistical analysis of dirty pictures. *Journal of the Royal Statistical Society B*, 48(3):259–302, 1986.
15. S. Geman and D. Geman. Stochastic relaxation, Gibbs distribution and the Bayesian restoration of images. *IEEE Transactions on Pattern Analysis and Machine Intelligence*, PAMI-6(6):721–741, November 1984.
16. D. Angwin and H. Kaufman. Image restoration using reduced order models. *Signal Processing*, 16:21–28, 89.
17. J. Besag. Spatial interaction and the statistical analysis of lattice systems. *Journal of the Royal Statistical Society B*, 36(2):192–225, 1974.
18. K. Ho. Exact probability-density function for phase-measurement interferometry. *Journal of the Optical Society of America*, 12(9):1984–1989, 1995.
19. K. S. Miller. *Complex Stochastic Processes. An Introduction to Theory and Applications*. Addison–Wesley Publishing Co., London, 1974.
20. E. Rignot and R. Chellappa. Segmentation of polarimetric synthetic aperture radar data. *IEEE Transactions Image Processing*, 1(1):281–300, 1992.

21. M. Grotschel, L. Lovasz, and A. Schrijver. *Beometric Algorithms and Combinatorial Optimization*. Algorithms and Combinatorics. Springer-Verlag, New York, 1988.
22. A Hassibi and S. Boyd. Integer parameter estimation in linear models with applications to gps. *IEEE Transactions on Signal Processing*, 46(11):2938–2952, Nov. 1998.
23. G. Strang and K. Borre. *Linear Algebra, Geodesy, and GPS*. Wellesley-Cambridge Press, New York, 1997.
24. L. Babai. On lovasz lattice reduction and the nearest lattice point problem. *Combinatorica*, 6:1–13, 1986.
25. T. Flynn. Two-dimensional phase unwrapping with minimum weighted discontinuity. *Journal of the Optical Society of America A*, 14(10):2692–2701, 1997.
26. J. Dias and J. Leitão. Interferometric absolute phase reconstruction in sar/sas: A bayesian approach. Thechical report, Instituto Superior Técnico, 2000.
27. D. Greig, B. Porteus, and A. Seheult. Exact maximum a posteriory estimation for binary images. *Jounal of Royal Statistics Society B*, 51(2):271–279, 1989.
28. Y. Boykov, O. Veksler, and R. Zabih. A new minimization algorithm for energy minimaization with discontinuities. In E. Hancock and M. Pelillo, editors, *Energy Minimization Methods in Computer Vision and Pattern Recognition-EMMCVPR'99*, pages 205–220, York, 1999. Springer.
29. M. Costantini. A novel phase unwrapping method based on network programing. *IEEE Transactions on Geoscience and Remote Sensing*, 36(3):813–821, May 1998.
30. R. Ahuja, T. Magnanti, and J. Orlin. *Network Flows: Theory, Algorithms and Applications*. Prentice Hall, 1993.
31. H. Ishikawa and D. Geiger. Segmentation by grouping junctions. In *Proceedings of the IEEE Computer Society Conference on Computer Vision and Pattern Recognition – CVPR'98*, pages 125–131, 1998.
32. R. Goldstein, H. Zebker, and C. Werner. Satellite radar interferometry: Two-dimensional phase unwrapping. In *Symposium on the Ionospheric Effects on Communication and Related Systems*, volume 23, pages 713–720. Radio Science, 1988.
33. H. Lim, W. Xu, and X. Huang. Two new practical methods for phase unwrapping. In *Proc. of the 1995 Internat. Geoscience and Remote Sensing Symposium*, pages 2044–2046, Lincoln, 1996.
34. W. Xu and I. Cumming. A region growing algorithm for insar phase unwrapping. In *Proceedings of the 1996 International Geoscience and Remote Sensing Symposium*, pages 196–198, Firenze, 1995.
35. T. Flynn. Consistent 2-D phase unwrapping guided by a quality map. In *Proceedings of the 1996 International Geoscience and Remote Sensing Symposium*, pages 2057–2059, Lincoln, NE, 1996.
36. D. Ghiglia and L. Romero. Roboust two-dimensional weighted and unweighted phase unwrapping that uses fast transforms and iterative methods. *Journal of the Optical Society of America*, 11(1):107–117, 1994.
37. M. Pritt. Phase unwrapping by means of multigrid techniques for interferometric SAR. *IEEE Transactions on Geoscience and Remote Sensing*, 34(3):728–738, May 1996.